

Ventilation and aerosolized drug delivery to the paranasal sinuses using pulsating airflow – a preliminary study*

Winfried Möller¹, Uwe Schuschnig², Gabriele Meyer³, Karl Häussinger⁴, Manfred Keller², Bernhard Junge-Hülsing⁵, Heribert Mentzel²

¹ Clinical Cooperation Group Inflammatory Lung Diseases, Helmholtz Zentrum München - German Research Center for Environmental Health, Gauting, Germany

² Pari GmbH, Munich and Starnberg, Germany

³ Department of Nuclear Medicine, Asklepios Hospital München-Gauting, Gauting, Germany

⁴ Department of Pulmonary Medicine, Asklepios Hospital München-Gauting, Gauting, Germany

⁵ Department of Otolaryngology, Hospital Starnberg, Starnberg, Germany

SUMMARY

Background: Although there is a high incidence of nasal disorders including chronic sinusitis, there is limited success in the topical drug delivery to the nose and the paranasal sinuses. This is caused by the nose being an efficient filter for inhaled aerosol particles and the paranasal sinuses being virtually non-ventilated.

Method: The objective of this study was to visualize the efficiency of sinus ventilation in healthy volunteers using dynamic ^{81m}Kr-gas imaging in combination with pulsating airflows. Furthermore, the deposition and retention of ^{99m}Tc-DTPA aerosol particles was assessed.

Results: The ventilation of the maxillary and frontal sinuses could be visualized by gamma camera imaging during pulsating airflow. In addition, using pulsating airflow, between 3% and 5% of nasally deposited aerosols penetrated into the paranasal sinuses while during application without pulsation aerosol deposition was below 1%. Furthermore pulsation increased aerosol deposition in the nasal airways by a factor of three.

Conclusions: The study demonstrates the high efficiency of a pulsating airflow in paranasal sinus ventilation and aerosolized drug delivery. This proves that topical drug delivery to the paranasal sinuses in relevant quantities is possible and indicates further clinical studies are necessary.

Key words: paranasal sinus ventilation, pulsating aerosol, krypton gas inhalation, scintigraphy

INTRODUCTION

Chronic sinusitis is one of the most commonly diagnosed chronic illnesses, and approximately 10-15% of the European and US population suffer from chronic rhinosinusitis⁽¹⁻³⁾. It is thought that inflammation of the nasal mucosa (i.e. rhinitis), due to bacterial, fungal or viral infections, allergies, or exposure to inhaled irritants, leads to acute sinusitis and chronic rhinosinusitis (CRS)^(3,4). Chronic inflammation of the nasal mucosa results in mucosal swelling, increased mucus secretion, loss of cilia, airway obstruction and blocked sinus drainage. Under these conditions, bacteria and viruses that are normally removed from the nasal cavity and sinuses by drainage of secretions may proliferate. This blockage of mucus drainage from the sinuses and reduced ventilation creates an environment for chronic rhinosinusitis^(3,5,6). In addition it was reported that impaired mucociliary clearance in patients with primary ciliary dyskinesia also causes chronic sinusitis⁽⁷⁻⁹⁾.

Genetic disposition may also play a role in the development of chronic rhinosinusitis⁽¹⁰⁾.

The paranasal sinuses are air-filled cavities in the bones of the skull surrounding the nose, ranging in volume between 5 ml and 30 ml⁽¹¹⁾. They communicate with the nose via narrow ducts – the ostia – of about 1-3 mm diameter and about 10-15 mm length^(11,12). Despite the fact that the sinuses are poorly ventilated hollow organs, in vivo and in vitro studies have shown that nebulized drugs can be deposited into the paranasal sinuses, although at very low efficiencies⁽¹³⁻¹⁸⁾. Therefore the primary option of treatment of chronic rhinosinusitis is surgery, often in combination with topical and systemic medical treatment^(3,19). An efficient topical therapy may allow treating upper respiratory diseases more effectively, prevent sinus surgery or at least extend the time span for sinus surgery. This hypothesis is supported by clinical data upon

nasal administration of Dornase alpha (Pulmozyme) via pulsating aerosol delivery (PARI SINUS) in cystic fibrosis patients⁽²⁰⁾.

Two physical mechanisms affect the transport of gas and aerosols into non-actively ventilated areas: diffusion and flow induction by pressure difference^(17,21,22). Flow induction by a pressure gradient has been found to be the most important mechanism for carrying particles into non-ventilated areas. Pulsating air flows or humming can be used to generate such pressure gradients. In spite of the widespread use of aerosols in respiratory diseases, only a few studies have been performed to assess ventilation and aerosol deposition into the paranasal sinuses^(14,17). In a previous study we could show the efficiency of Kr-gas ventilation to the paranasal sinuses and aerosolized drug delivery in a nasal cast using pulsating airflows^(23,24).

The objective of this study was to investigate sinus ventilation in three healthy human volunteers with normal nasal anatomy using dynamic ^{81m}Kr-gas imaging in combination with pulsating airflows. Furthermore the deposition efficiency of radiolabeled DTPA aerosol (diethylene triamine pentaacetic acid) was assessed. Besides retention during 24 hours the fraction of DTPA translocating to circulation was investigated with and without pulsation.

MATERIALS AND METHODS

Human volunteers

Three male healthy non-smoking volunteers with mean age 46 ± 12 years participated in the study. The subjects had normal lung function and no history of allergic diseases. Normal nasal anatomy was confirmed by MRT imaging and fiber optic rhinoscopy prior to the study. Nasal resistance was measured before and after application of a nasal decongestant containing 0.05% oxymetazoline using the Masterscreen Rhino (Jaeger GmbH, Hoechberg, Germany). In the three subjects baseline nasal resistance was 0.24 ± 0.21 kPa/(l/s) (mean \pm standard deviation, pressure 150 Pa) and it decreased by a factor of two, 10 min after the application of the nasal decongestant. The study protocol was approved by the Ethical Committee of the Medical School of the Ludwig Maximilian University (Munich, Germany), and informed consent was obtained from each subject. Prior to gas/aerosol delivery, 2 puffs of a nasal decongestant pump spray containing 0.05% oxymetazoline were applied to the nose to enlarge the nasal airways. ^{81m}Kr-gas ventilation and aerosol delivery were studied without and with pulsation on separate occasions in each subject.

Pulsating aerosol delivery system

A pulsating aerosol was generated using the PARI SINUS system (Pari GmbH, Starnberg, Germany). It is based on a PARI BOY N aerosol drug delivery device^(22,23). The compressor has an integrated pressure wave generator driven by the same motor. The pressure wave had a 45 Hz frequency with amplitude of 25 mbar (measured with a pressure transducer inside

the model). It was attached via a tubing connector to the vent opening of a PARI LC SPRINT Junior jet nebulizer in order to superimpose the pressure wave on the aerosol flow. The mass median aerodynamic diameter (MMAD) of the aerosol generated by the PARI LC SPRINT Junior jet nebulizer was $3.2 \mu\text{m}$ with a geometric standard deviation of 2.6. The rate of mass output was 0.2 ml/min, and there was no significant difference in output rate with or without pulsation. For gas/aerosol delivery to the nose the nebulizer was coupled to the right nostril and the left nostril was coupled via a flow resistor to output tubing. During delivery the subject closed his soft palate, which directed the aerosol to the output nostril and prevented gas/aerosol penetration to the lung.

Kr-gas ventilation studies

Kr-gas was continuously ventilated through the nasal airways in front of a single-head gamma camera (DIACAM, Siemens, Erlangen, Germany), using the PARI SINUS pulsating drug delivery system. The air supply of the PARI SINUS was directly taken from the ^{81m}Kr-gas generator output channel. The head of the gamma camera was equipped with a medium-energy collimator. Kr-gas ventilation imaging was performed with and without pulsation. Serial images (2 frames per second) were recorded from the anterior view. This allowed dynamic studies of filling and emptying of the nose including the sinuses. The gamma camera images were analyzed using the ImageJ 1.30 software package (<http://rsb.info.nih.gov/ij/>). For analysis of the distribution of the ^{81m}Kr-gas to the different compartments all serial images were superimposed (Figure 1). Regions of interest (ROI) of the nasal airways and the sinuses were defined as shown in Figures 1A and 1C, and the activity was obtained in these ROI's. For background activity correction serial images were recorded without Kr-gas delivery. In a nasal cast study we could show that interchange of the nebulizer between right/left nostrils had no influence on ^{81m}Kr-gas sinus ventilation efficiencies⁽²³⁾.

Aerosol inhalation studies

An aerosol was generated using a solution composed of ^{99m}Tc-DTPA (Pentacis, Schering, Germany). DTPA (diethylene triamine pentaacetic acid) is a nanocolloid of 500 Dalton size. In nuclear medicine DTPA aerosols are used for ventilation imaging and the measurement of the alveolar transmembrane permeability⁽²⁵⁾. ^{99m}Tc-DTPA clears out of the lungs into circulation by passive diffusion through the intercellular junctions of the alveolar-capillary barrier with a half time of about 90 min. Four milliliters of DTPA solution containing about 600 MBq of ^{99m}Tc-activity were added to the nebulizer. For nasal aerosol delivery the nebulizer was coupled to the right nostril, while a PALL output filter including a flow resistor (PALL BB50 filter, Pall Corporation, New York, NY, USA) was coupled to the left nostril, and the aerosol was delivered for 20 sec, while the subject closed his soft palate. Nebulizer and output filter were then interchanged between left and right nostril and the

aerosol was delivered for another 20 sec. Prior to aerosol delivery the output rate of the nebulizer was measured by collecting all particles on a PALL BB50 filter. From the nebulizer output rate and the activity deposited on the output filter the total nasal deposition rate was assessed.

Nasal deposition, retention and clearance were measured during 24 hours post DTPA delivery using planar gamma camera imaging (Diacam, Siemens, Erlangen, Germany) in combination with a low energy collimator. Anterior and lateral gamma

camera images were recorded directly after inhalation as well as 1.5 h, 3 h, 6 h and 24 h post inhalation. Subjects spent the night at their homes and returned to the site the next morning for recording the 24 h image. Urine was collected during 24 hours and the fraction of DTPA translocated to the blood was assessed by activity analysis in urine. The subjects sat in front of the gamma camera head, which was positioned in the upright format, allowing a simultaneous imaging of the nose and the upper lung. Count rates in selected regions of interest (ROI's) were analyzed using the ImageJ software package.

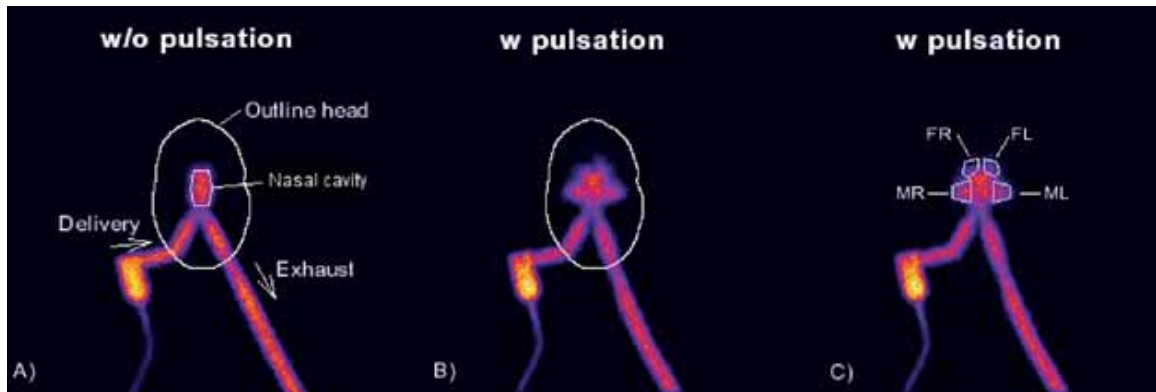


Figure 1. Nasal ^{81m}Kr -gas imaging without (w/o, A) and with (w, B and C) pulsating airflow in front of the gamma camera. The nebulizer coupled to the right nostril and the exhaust tubing coupled to the left nostril is shown. Regions of interest of the nasal cavity (A) and of the right and left maxillary and frontal sinuses (MR, FR, FL and ML) are shown (C).

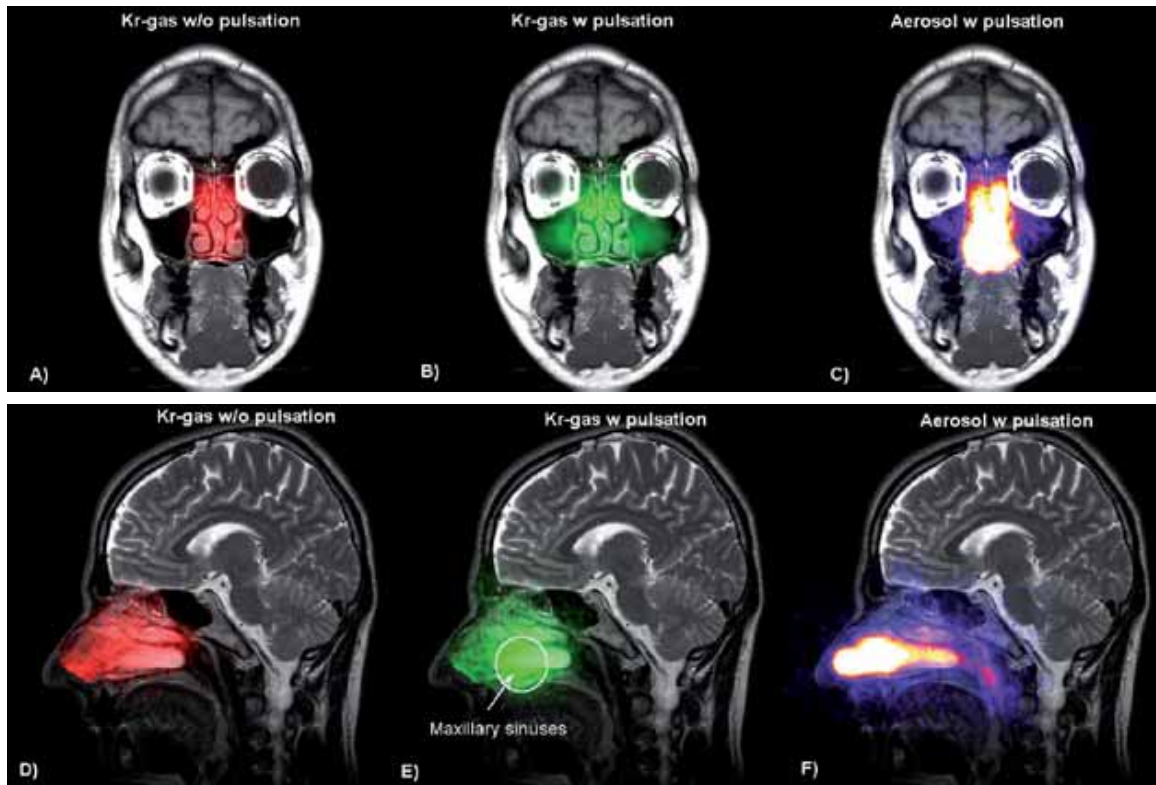


Figure 2. A) and B) superposition of anterior gamma camera images of ^{81m}Kr -gas ventilation w/o and w pulsating airflow with a coronal MRT slice in one subject. C) Superposition of gamma camera image of aerosol inhalation w pulsating airflow with MRT head image in one subject. D) - F) similar superposition of lateral gamma camera images with a sagittal MRT slice.

ROI's generated from previous ^{81m}Kr ventilation images were used and included the nasal airways and the sinuses. Count rates were corrected for background activity and for radioactive decay in both the deposition and retention images and the urine activity analysis. Group differences between delivery w/o and w pulsation were calculated by a two-sided t-Test (Winstat software package for Microsoft Excel, Version 2005.1, www.winstat.com), using a significance level of $p < 0.05$.

RESULTS

Kr-gas ventilation

Kr-gas ventilation images obtained with (w) and without (w/o) pulsation are shown in Figure 1. Figures 1A represents Kr-gas ventilation w/o pulsation. Only the central nasal cavity appears on the image and the distribution was used to define the nasal cavity (nasal-AW) region of interest (ROI). In addition the delivery system is shown with the nebulizer coupled to the right nostril, as well as the exhaust tubing coupled to the left nostril. The sinuses do not appear on this image, suggesting that there is little Kr-gas penetration to the paranasal sinuses. Figure 2A shows the superposition of the Kr-gas activity distribution w/o pulsation with the MRT-image of one subject, which shows negligible Kr-gas activity in the maxillary sinuses. Figures 1B and 1C illustrate the Kr-gas activity distribution w pulsation, where in contrast to Figure 1A, the maxillary sinuses clearly display as activity areas left and right to the nasal airways. The superposition of Kr-gas activity with a MRT-image in Figure 2B and 2E shows the penetration of Kr-gas into the maxillary sinuses with pulsating airflow. Figure 1B was used to analyze the horizontal and the axial activity distribution, as shown in Figure 3 and to define ROI's of the four sinus cavities, as illustrated in Figure 1C (MR and ML – maxillary right and left sinuses, FR and FL – frontal right and left sinuses; the frontal sinuses include ethmoid and sphenoid sinuses). The horizontal activity distribution shown in Figure 3A demonstrates the activity appearance lateral (left and right) to the nasal airways with pulsating airflow. This additional activity represents Kr-gas penetration to the right and left maxillary sinuses (MR and ML). Figure 3B represents the activity distrib-

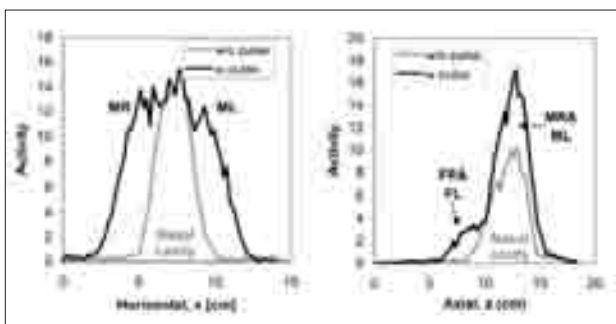


Figure 3. Lateral (A) and axial (B) ^{81m}Kr -gas activity distribution above the nasal cavity without (w/o) and with (w) pulsating airflow. Activity accumulation in maxillary (MR and ML) and frontal (FR and FL) sinuses is highlighted.

ution obtained from a lateral image (Figure 2D and 2E) along a vertical axis (axial), covering the frontal sinuses, the nasal cavity and the maxillary sinuses. Without pulsation there is only Kr-gas penetration to the nasal airways, while with pulsation Kr-gas penetration to the frontal sinuses adds activity above the nasal airways and Kr-gas penetration to the maxillary sinuses adds activity to the central nasal cavity region and below. Based on the ROI's defined from Figures 1A and 1C the mean Kr-gas activity in the central nasal cavity and the frontal and maxillary sinuses is shown in Figure 4 for the three volunteers involved in the study. After normalization of the activity to the nebulizer activity there is no difference in activity in the central nasal cavity-ROI due to pulsating airflow. However, there is more than a fivefold increase of activity in the four sinuses with pulsating airflow.

Figure 5 shows the wash-out characteristics with pulsation after switching off the Kr-gas delivery. The drop in activity for the nebulizer was much faster compared to that in the nasal airways or in the sinuses. In addition there was a delay in Kr-gas wash-out from the sinuses compared to the nasal airways.

Aerosol deposition in the nasal airways and in the nasal sinuses

The first image recorded immediately after aerosol delivery did not show aerosol deposition in the chest region, which confirms tight closure of the soft palate during aerosol delivery. Total aerosol deposition (% of nebulized dose) in the nasal cavity of the three subjects was $25 \pm 16\%$ without pulsation and $58 \pm 17\%$ with pulsation ($p < 0.01$). With pulsation $4.2 \pm 0.3\%$ of activity deposited in the nose penetrated to the sinuses while it was below 1% without pulsation.

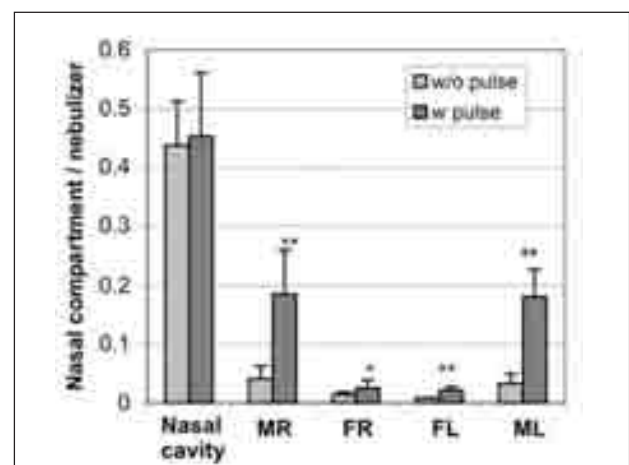


Figure 4. ^{81m}Kr -gas activity accumulation in the central nasal region and in the maxillary and frontal sinuses (MR, FR, FL, ML) without (w/o) and with (w) pulsating airflow, normalized to activity in the nebulizer (mean \pm standard deviation of three volunteers, significance of difference between w/o and w pulsation: *: $p < 0.05$, **: $p < 0.01$).

DTPA clearance from the nasal cavity

Figure 6A shows the mean retention of nasally deposited DTPA with and without pulsation in the three volunteers. Both, for delivery without and with pulsation, about 30% of the deposited aerosol are cleared with a half-time of 1 hour. The remaining fraction was cleared with half-times of 6.9 and 7.9 hours without and with pulsating aerosol delivery, respectively. After 24 hours $5.4 \pm 1.8\%$ and $8.6 \pm 1.3\%$ of initially deposited activity were retained in the nasal cavity without and with pulsation, respectively. Figure 6B shows the clearance of activity deposited in the total nose and in the sinuses in one volunteer: $4.2 \pm 0.3\%$ of activity deposited in the nose penetrated to the sinuses and the parallel decay of activity with time shows similar clearance behavior of the DTPA aerosol from the sinuses, as was recorded from the whole nasal cavity.

DTPA translocation to circulation

Of the activity deposited in the nose, $17.7 \pm 2.0\%$ and $5.6 \pm 0.4\%$ with and without pulsation, respectively ($p < 0.01$), were excreted into the urine within 24 hours. The higher fraction of DTPA penetrating to the blood with pulsating airflow correlates with a higher total deposition.

DISCUSSION

The inefficiency of ventilation of the paranasal sinuses using standard inhalation devices has been demonstrated by the 133-Xenon washout technique^(26,27). Typical gas exchange half-times are 10 to 30 min in healthy subjects, and further increased in patients with sinus diseases. This is not sufficient to transport significant amounts of drugs into the paranasal sinuses in order to perform a topical therapy. This efficiency can be significantly enhanced using pulsating airflow.

Kr-gas sinus ventilation

The efficiency of pulsating airflow for proper sinus ventilation is evident from Figures 1 to 3. Without pulsation, less than

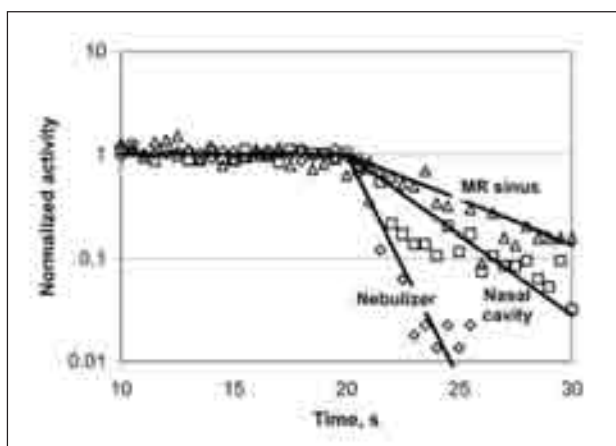


Figure 5. Wash-out characteristics of the activity from the nebulizer, the nasal airways and the right maxillary sinus after switching off the ^{81m}Kr -gas delivery at $T = 20$ s.

10% of the total Kr-gas activity within the nasal cavity penetrated the sinuses. This rate increased to about 48% with pulsation. This demonstrates that generation of significant pressure differences at the ostium openings leads to increased gas transport into the sinuses. Similar results could be confirmed in a previous study in a nasal cast⁽²³⁾. In the cast study various configurations of sinus volumes and ostium diameters were tested. There were optimal combinations of ostium diameter and sinus volume for maximal sinus ventilation with pulsation. The worst configuration was that of large (5 mm) ostium diameters, while ostium diameters of two and three millimeters were most efficient for sinus ventilation in conjunction with pulsating airflow. These optimum conditions of ventilation of the sinuses may reflect a resonance behaviour, since an ostium including a sinus cavity can be considered as a Helmholtz-resonator-like configuration. However, experimental and simulation investigations show resonance conditions for similar configurations of ostium diameter and sinus volume at higher pulsation frequencies of above 100 Hz, while our device operates at 45 Hz^(11,17).

Pulsating airflow caused a sustained release of ^{81m}Kr -gas activity from the nasal airways and the sinuses after switching off the radioactive gas delivery. As can be seen from Figure 5 the activity drop was much slower in the nasal airways compared to that in the nebulizer, and was further slowed in the sinus cavities. This indicates a delay in gas exchange between sinuses and nasal airways. This delay can cause an increased residence time of an aerosol drug in the sinuses and this can further enhance the aerosol deposition fraction, both in the nasal airways and in the sinuses. Paranasal sinus wash-out without pulsation is much slower than with pulsation, as has been shown using 133-Xenon scintigraphy⁽²⁶⁾.

Nasal aerosol deposition

Access and deposition of significant amounts of aerosol into the sinuses could not be detected without pulsation, and with pulsation only about 4.5% of activity deposited in the nasal cavity was detected in the sinus ROI's. This rate is low com-

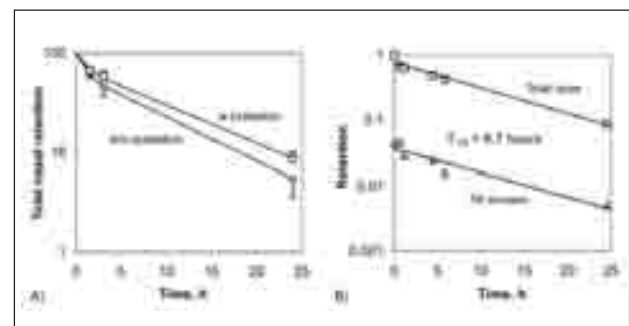


Figure 6. A) Clearance of ^{99m}Tc -DTPA aerosol from the nasal cavity without (w/o) and with (w) pulsating airflow. B) Clearance of ^{99m}Tc -DTPA aerosol from the nasal cavity and the sinuses with pulsating airflow in one subject.

pared to Kr-gas ventilation efficiency and may result from high aerosol deposition at the nasal entrance site (nasal valve, see Figure 2F). Experimental and computational predictions of particle deposition in the human nasal cast model and anatomical replicas support the assumption that there is an efficient nasal filtration effect with high deposition at the nasal vestibule, nasal valve and anterior turbinates^(18,28). Increasing aerosol deposition efficiency may be achieved by further reduction of the particle size of the aerosol. This rate is in the range of results obtained in our previous *in vitro* study using a nasal cast, where up to 8% of the nebulized dose could be deposited in the paranasal sinuses⁽²³⁾. Nevertheless, 4.5% deposited dose in the sinuses may provide sufficient amount of drug for a first step topical aerosol therapy. Using the PARI SINUS device a one-minute delivery would deposit about 5 mg of nebulized solution in the sinuses.

Besides aerosol transport to the sinuses, pulsation enhanced aerosol deposition in the nasal cavity more than twofold. Increased intranasal aerosol deposition by pulsating airflow was shown before⁽¹³⁾. This enhanced aerosol deposition in the nasal airways may be advantageous for the treatment of nasal diseases other than sinusitis, such as bacterial or fungal infections or chronic inflammation of the nasal airways, and would offer alternative treatment options with less side effects compared to those described for the treatment of fungal sinusitis and complications of rhinosinusitis⁽⁴⁾.

DTPA clearance from the nasal airways

In addition to higher aerosol deposition efficiencies, drug delivery with pulsation is associated with slower clearance of the radiotracer from the nose, suggesting penetration into the nose to sites with retarded mucociliary clearance, as for example the anterior nasal cavity, olfactory bulb or the paranasal sinuses. Suman reported between 25% and 40% clearance of nasally administered DTPA aerosol within 30 min from a nasal spray pump and nasal nebulizer, respectively⁽²⁹⁾. This faster clearance may result from higher deposition characteristics in the ciliated regions of the nose due to larger particles, originating from the nebulizer and spray pump devices. In addition, the nasal decongestant administered in our study may influence ciliary activity. But *in vitro* and *in vivo* studies suggest a minor influence of the doses of oxymetazoline used in our study on ciliary beat frequency and mucociliary transport rate^(30,31). Both, with and without pulsation, there was retained activity in the nose after 24 hours, where the delivery with pulsation was associated with a higher fraction. Assuming that mucociliary clearance removes all particles within 24 hours, this data suggests a fraction of particles was retained in the nose longer than 24 hours. A similar phenomenon has been observed in the human airways⁽³²⁾, and the physiological mechanisms of this long-term retention are not clear. Mechanisms discussed include areas of retarded mucus transport or particle deposition between cilia. The clearance kinetics

in the range of hours can provide longer residence times for a drug administered as an aerosol to the nose and it prevents rapid removal by circulation, therefore allowing formulations with sustained release profiles and possibly once daily application even when their half time values are shorter.

DTPA translocation to circulation

Pulsating aerosol delivery enhanced the fraction of activity deposited in the nose being excreted into urine within 24 hours. DTPA deposited onto the alveolar lung epithelium penetrates into the circulation and is excreted into urine within 24 hours⁽³³⁾. In contrast DTPA deposited onto mucus is primarily cleared by mucociliary transport because of the high affinity of DTPA to mucus^(34,35). Therefore the fraction of DTPA excreted into urine may reflect aerosol deposited onto nasal mucosa, which is not covered by mucus at the period of delivery. Such areas are also known from small airways in the lung⁽³⁶⁾. In small airways mucus does not appear as a continuous layer, rather it is transported as plugs. In larger airways and in the trachea these plugs merge to a continuous mucus layer. Therefore, there are transiently areas in small airways and in the nasal cavity, which are free of a mucus layer. With respect to DTPA transport these areas may behave similarly as the alveolar epithelium and maintain uptake into blood circulation. The higher fraction of DTPA penetrating to blood with pulsating airflow correlates with a higher total deposition. This may result from a deeper penetration of the aerosol into the nasal cavity and deposition onto the nasal mucosa, which is, to a lower extent covered by mucus, thus potentially allowing for absorption.

Durand et al.⁽³⁷⁾ used a more realistic plastinated nasal cast of a human cadaver and measured aerosol deposition by gamma camera imaging, with and without sounding airflow. Using sounding airflow they could confirm activity penetration into the sinuses, but only just above the gamma camera background activity. They did not give any estimation on absolute deposition efficiencies in their study. Maniscalco et al.⁽¹⁷⁾ could also show that sounding airflow (humming) causes an increase in sinus drug deposition in human volunteers, enhancing the delivery of a nitric oxide-synthase inhibitor to the nasal sinuses and thereby reducing the release of nasal NO during humming. Drug delivery without sounding airflow had no effect on nasal NO release.

Opportunities for the aerosol treatment of nasal disorders

The data presented in this study are limited to subject with normal nasal anatomy and the nasal airways were decongested, therefore the results may not directly be applicable to patients with chronic rhinosinusitis. Nasal obstructions in patients with rhinosinusitis and complete closure of ostia may prevent gas and aerosol penetration to the sinuses. In addition the complex structure of the nasal airways causes high particle deposition at the nasal valve and the nasal turbinates, especially of larger

particles⁽³⁸⁾. This makes the nose an efficient filter for inhaled pollutants. However, it also significantly reduces the amount of aerosol penetrating to areas where there is access to the sinus cavities. This is a limiting factor in most of the studies published in relation to aerosolized nasal or sinus drug delivery. Although 4.5% aerosol deposition in the nasal sinuses appears low, it may provide sufficient drug delivery for a topical inhalative aerosol therapy, but the efficiency of the system in patients suffering from chronic sinusitis has to be shown in future clinical trials.

Nevertheless patients with nasal airway obstructions caused either by nasal polyps or by the inflamed mucosa, such as patients with chronic sinusitis, may benefit from aerosolized drug delivery using pulsating airflows⁽³⁹⁾. However, a principal limitation of aerosol drug delivery to the sinuses is that ventilation has to be possible. Obstructed sinuses did not show enhanced NO release after humming, as was shown by Lundberg et al.⁽⁴⁰⁾. Nevertheless these patients may benefit from pulsating aerosol delivery by an increased aerosol deposition in the nasal cavity with subsequent redistribution of the drug due to extended retention of the drug in the nasal cavity. This is supported by preliminary clinical data in CF patients after nasal administration of Dornase alpha (Pulmozyme) using pulsating airflow⁽²⁰⁾.

REFERENCES

1. Van Cauwenberge P, Watelet JB. Epidemiology of chronic rhinosinusitis. *Thorax* 2000; 55: 20S-1.
2. MedlinePlus. Sinusitis Fact Sheet, January 2006. Washington, DC: National Institute of Allergy and Infectious Diseases; 2006 [updated 2006; cited]; Available from: <http://www.niaid.nih.gov/factsheets/sinusitis.htm>.
3. Fokkens W, Lund V, Mollol J. The European Position Paper on Rhinosinusitis and Nasal Polyps (EP3OS) group. *Rhinology* 2007; 45: Suppl 20: 1-137.
4. Epstein VA, Kern RC. Invasive fungal sinusitis and complications of rhinosinusitis. *Otolaryngol Clin North Am* 2008; 41: 497-524.
5. Clement PA. Definitions of sinusitis. *Acta Otorhinolaryngol Belg* 1997; 51: 201-2003.
6. Baraniuk J, Maibach H. Pathophysiological classification of chronic rhinosinusitis. *Respir Res* 2005; 6: 149.
7. Armengot M, Juan G, Barona R, Garin L, Basterra J. Immotile cilia syndrome: nasal mucociliary function and nasal ciliary abnormalities. *Rhinology* 1994; 32: 109-111.
8. Min YG, Shin JS, Choi SH, Chi JG, Yoon CJ. Primary ciliary dyskinesia: ultrastructural defects and clinical features. *Rhinology* 1995; 33: 189-193.
9. Noone PG, Leigh MW, Sannuti A, et al. Primary ciliary dyskinesia - Diagnostic and phenotypic features. *Am J Respir Crit Care Med* 2004; 169: 459-467.
10. Pinto JM, Hayes MG, Schneider D, Naclerio RM, Ober C. A genomewide screen for chronic rhinosinusitis genes identifies a locus on chromosome 7q. *Laryngoscope* 2008; 2008; 118: 2067-2067.
11. Tarhan E, Coskun M, Cakmak O, Celik H, Cankurtaran M. Acoustic rhinometry in humans: accuracy of nasal passage area estimates, and ability to quantify paranasal sinus volume and ostium size. *J Appl Physiol* 2005; 99: 616-623.
12. Jones N. The nose and paranasal sinuses physiology and anatomy. *Adv Drug Deliv Rev* 2001; 51: 5-19.
13. Sato Y, Hyo N, Sato M, Takano H, Okuda S. Intra-nasal distribution of aerosols with or without vibration. *Z Erkr Atmungsorgane* 1981; 157: 276-280.
14. Hyo N, Takano H, Hyo Y. Particle deposition efficiency of therapeutic aerosols in the human maxillary sinus. *Rhinology* 1989; 27: 17-26.
15. Suman JD. Nasal drug delivery. *Expert Opin Biol Ther* 2003; 3: 519-523.
16. Saijo R, Majima Y, Hyo N, Takano H. Particle deposition of therapeutic aerosols in the nose and paranasal sinuses after transnasal sinus surgery: a cast model study. *Am J Rhinol* 2004; 18: 1-7.
17. Maniscalco M, Sofia M, Weitzberg E, Lundberg JO. Sounding airflow enhances aerosol delivery into the paranasal sinuses. *Eur J Clin Invest* 2006; 36: 509-513.
18. Kimbell JS, Segal RA, Asgharian B, et al. Characterization of Deposition from Nasal Spray Devices Using A Computational Fluid Dynamics Model of The Human Nasal Passages. *J Aerosol Med* 2007; 20: 59-74.
19. Gosepath J, Mann WJ. Current Concepts in Therapy of Chronic Rhinosinusitis and Nasal Polyposis. *ORL* 2005; 67: 125-136.
20. Mainz J, Mentzel HJ, Schneider G, et al. Sinu-nasal inhalation of Dornase alpha in CF. Results of a double-blind placebo-controlled pilot trial. *J Cystic Fibrosis* 2008; 7: S27.
21. Kauf H. Eindringvermögen von Aerosolen in Nebenräume [Penetration ability of aerosols into secondary spaces]. *Eur Arch Otorhinolaryngol* 1968; 190: 95-108.
22. Böhm A, Luber M, Mentzel H, Knoch M. Investigating Drug Delivery to the Sinuses: An In Vitro Deposition Study Using a Nasal Cast Model. *Respiratory Drug Delivery IX* 2004; 3: 601-604.
23. Möller W, Schuschnig U, Meyer G, Mentzel H, Keller M. Ventilation and drug delivery to the paranasal sinuses: studies in a nasal cast using pulsating airflow. *Rhinology* 2008; 46: 213-220.
24. Schuschnig U, Keller M, Klopfer E, et al. Drug Delivery to the Nasal and Paranasal Cavities - Critical Cast Dimensions and Aerosol Dynamics. In: Dalby RN, Byron PR, Peart J, Suman JD, Farr SJ, Young PM, editors. *Respiratory Drug Delivery 2008* Arizona. Scottsdale, Arizona, USA: Virginia Commonwealth University; 2008. p.227-238.
25. Wagner HN, Szabo Z, Buchanan J. Principles of nuclear medicine. 2nd ed. Philadelphia: Saunders; 1995.
26. Paulsson B, Dolata J, Larsson I, Ohlin P, Lindberg S. Paranasal sinus ventilation in healthy subjects and in patients with sinus disease evaluated with the 133-xenon washout technique. *Ann Otol Rhinol Laryngol* 2001; 110: 667-674.
27. Paulsson B, Lindberg S, Ohlin P. Washout of 133-xenon as an objective assessment of paranasal sinus ventilation in endoscopic sinus surgery. *Ann Otol Rhinol Laryngol* 2002; 111: 710-717.
28. Schroeter JD, Kimbell JS, Gross EA, et al. Application of Physiological Computational Fluid Dynamics Models to Predict Interspecies Nasal Dosimetry of Inhaled Acrolein. *Inhal Toxicol* 2008; 20: 227-243.
29. Suman JD, Laube BL, Dalby R. Comparison of nasal deposition and clearance of aerosol generated by nebulizer and an aqueous spray pump. *Pharm Res* 1999; 16: 1648-1652.
30. Inanli S, Ozturk O, Korkmaz M, Tutkun A, Batman C. The effects of topical agents of fluticasone propionate, oxymetazoline, and 3% and 0.9% sodium chloride solutions on mucociliary clearance in the therapy of acute bacterial rhinosinusitis in vivo. *Laryngoscope* 2002; 112: 320-325.
31. Luo Z, Han D, Xiaohong S, Kuiji W, Hong W. Effect of Oxymetazoline on healthy human nasal ciliary beat frequency measured with high-speed digital microscopy and mucociliary transport time. *Ann Otol Rhinol Laryngol* 2008; 117: 127-133.
32. Möller W, Häussinger K, Winkler-Heil R, et al. Mucociliary and long-term particle clearance in the airways of healthy non-smokers. *J Appl Physiol* 2004; 97: 2200-2206.
33. Köhn H, König B, Klech H, Pohl W, Mostbeck A. Urine excretion of inhaled technetium-^{99m}-DTPA: an alternative method to assess lung epithelial transport. *J Nucl Med* 1990; 31: 441-449.

34. Cheema MS, Groth S, Marriott C. Binding and diffusion characteristics of ^{14}C EDTA and $^{99\text{m}}\text{Tc}$ DTPA in respiratory tract mucus glycoprotein from patients with chronic bronchitis. *Thorax* 1988; 43: 669-673.
35. Bennett WD, Ilowite JS. Dual pathway clearance of $^{99\text{m}}\text{Tc}$ -DTPA from the bronchial mucosa. *Am Rev Respir Dis* 1989; 139: 1132-1138.
36. Van As A, Webster I. The morphology of mucus in mammalian pulmonary airways. *Environ Res* 1974; 7: 1-12.
37. Durand M, Rusch P, Granjon D, et al. Preliminary study of the deposition of aerosol in the maxillary sinuses using a plastinated model. *J Aerosol Med* 2001; 14: 83-93.
38. Schroeter JD, Kimbell JS, Asgharian B. Analysis of particle deposition in the turbinate and olfactory regions using a human nasal computational fluid dynamics model. *J Aerosol Med* 2006; 19: 301-313.
39. Knipping S, Holzhausen H, Riederer A, Bloching M. Cystic fibrosis: ultrastructural changes of nasal mucosa. *Eur Arch Otorhinolaryngol* 2007; 264: 1413-1418.
40. Lundberg JO, Maniscalco M, Sofia M, Lundblad L, Weitzberg E. Humming, Nitric Oxide, and Paranasal Sinus Obstruction. *JAMA* 2003; 289: 302-303.

Dr. Winfried Möller
Helmholtz Center Munich - German Research Center for
Environmental Health
Clinical Cooperation Group Inflammatory Lung Diseases
Robert-Koch-Allee 29
D-82131 Gauting
Germany

Tel: + 49-89-3187 1881

Fax: + 49-89-3187 191881

E-mail: moeller@helmholtz-muenchen.de